TECHNICAL UNIVERSITY OF CLUJ-NAPOCA

ACTA TECHNICA NAPOCENSIS

Series: Applied Mathematics, Mechanics, and Engineering
Vol. 65, Issue II, June, 2022

COMPUTATIONAL ANALYSIS OF THE FLOW PHYSICS OVER A RECTANGULAR OPEN CAVITY WITH VARYINGS SHOCK IMPINGEMENTS

Tanmay B. GHOLAP, Majella Riona R., Adithya M., Deepthi Chowdary BOLLA and Devabrata SAHOO

Abstract: *In aviation, open cavities have a critical role in influencing performance characteristics. Components such as combustion chamber, landing gear, and weapon bays contain a cavity influenced by the shear layer. Supersonic conditions of cavity flows are a prerequisite for the configuration of missiles and future aerospace vehicles. In the present research, the stream passing above a rectangular open pit containing a shear layer is computationally studied after the impingement of an oblique shock wave generated by a wedge type shock generator. The cavity duct investigated in the present study has a length to depth ratio of 3 at zero degrees angle of attack. Investigation on the influence of flow characteristics such as the magnitude of drag, pressure distribution, and recirculation within the duct has been performed and analyzed for cases in the presence and absence of shock generator at Mach 3. No particular disruption of the shear layer occurs in the absence of an oblique shock. However, a robust recirculation in the shock impingement cases is observed. The shear layer lifts up due to the thrust force generated in the open cavity on the impingement of a shock wave. A strong rear shock is generated at the rear wall separation point of the open duct. Further, the effect of the rise in the strength of the impinging shock on the entire flow over the cavity is also investigated. As the strength of impinging shock increases, it was observed that the magnitude of pressure distribution on the cavity surface also increases.*
Key words: *Supersonic Flows, Rectangular Open Cavity, Shear Layer, Shock Impingement, Shock Generator.*

1. INTRODUCTION

Flow over a cavity is gaining importance for both practical and analytical interests. These interests present plane objectives in flame holders, wheel wells and weapon bay doors of aircraft, pipe fittings, and halfway avoided folds or sunroofs in road vehicles. In the case of the configuration of aviation vehicles, cavities are proven to be a boon owing to their drag attributes. A grasp on the complete knowledge of the impact caused in numerous air vehicles despite their streamlined shape is the basic requirement while employing the cavity design. Cavity shows up on the airplane as sabot and landing gear wheel wells, on shots having outside rifling, or on shots of dispatched caliber. Apart from the cases of single holes mentioned above, the occurrence of double holes or pits can also be observed. The presence of such pits affects acoustic execution while influencing the streamlined shape of the body of the aircraft. In addition to this, the presence of a cavity wall affects the stealth abilities of an aircraft. The shear layer flowing across a cavity makes a design possible for flow detachment and reattachment. The fluctuation of stream in the open duct flow affected by the shear layer owing to an extensive array of flow conditions tends to be the focal point. Fluctuations in the flow field occurring generate adverse effects on the performance and aerodynamic stability, as damages are caused to sensitive instruments and structural loading. Figure 1 shows the flow around an open duct with an extent to altitude ratio of 3. From the figure, it can be observed that the cavity is filled by a recirculation zone and mixing layer does not go into the open pit but partial stream penetration takes place. Shear layer thickens as it moves from the fore wall

Received: 30.04.22; **Similarities**: 18.05.22: **Reviewed**: 06.06./26.05.22: **Accepted**:21.06.22.

corner to the aft wall corner. Flow expansion takes place at the front wall top corner point, whereas, a rear weak shock formation is generated at the rear wall corner point. Compression of flow leads to this shock formation. The thickness of the boundary layer impending is of the order of duct's depth.

McGregor and White [1] conducted experimental studies and analytical considerations to solve cavity problems in both high and low Mach numbers which began for the designers' knowledge for its usage. They observed that the shear layer extending above the duct deflects when the cavity resonates. At the rear wall corner of the pit, the shear layer recompression pressure was tracked to find the amplitude of this deflection. At one or more Mach numbers, all the different types of cavities taken were found to be resonated. The drag on the cavity was observed majorly influenced by the results of cavity resonance through a major span of variables. In the case of internal flow at subsonic speeds, this resonance can amplify the drag by 250%. Edwards and Zhang [2] reported that distortion in the flow decreases with increasing Mach number in supersonic cavity cascade flow. The acoustic and aerodynamic characteristics are different than that of single cavity flow. The higher levels of vibrational modes in the dense boundary layer are complex to examine. As the flow progresses downstream, the prevalent oscillation frequency transitions from higher recurring modes to lower ones. The shear layer gets highly excited while moving downstream. Zhang and Edwards [3] carried out computational analysis on a duct having an extent to height ratio 3 using a two-layer eddy viscosity model. They observed the oscillations were longitudinal and not fully acoustic-driven, rather, a fluid dynamics mechanism directed the entire flow. The distribution of flow-field before the duct and the shear layer's swirling motion begins on the duct fore wall. At Mach 2.5, the trailing edge vortex is powerful at the aft region of the cavity. The open cavity contains two recirculation zones in the corner regions. Baysal and Stallings [4] performed experimental and computational tests for open, closed, and translational pits of extent to height correspondence of 6, 12, and 16 at Mach 1.5. They reported that the fundamental characteristics of the oscillations are influenced by the shear layer formed for different L/D ratios. The drag coefficient on the cavity increased as the length of the cavity increased. Gruber et al. [5] studied open cavities with varying aft ramp angles and offset ratios by investigating it in an experimental and computational manner. The duct's rear wall gradient angle has a major role in the determination of the shear layer which travels along the pit's span. For an offset, one with a rear ramp wall slope of ninety degrees, the compression wave occurs when the flow is separated from the front wall's cavity corner and a strong recompression shock is generated at the rear wall. As the ramp wall angle is changed from 90 to 16 degrees, the shape of the recompression shock also changes marginally. Rowley et al. [6] carried out numerical computations to showcase the flow past an open cavity. Wake mode and shear layer modes were

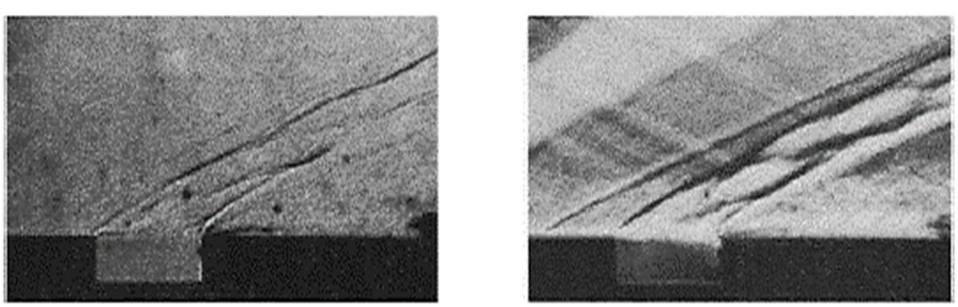

Fig. 1. Shadowgraph (left) and schlieren (right) images of flowfield around a cavity configuration of L/D = 3. L illustrates the length and D portrays the altitude of the pit. Ramp wall angle of the of the cavity is 90 degrees Gruber et al. [5].

analyzed for the subsonic flow. For lesser depth, low Reynolds, and Mach numbers, the flow is steady.As the variables increase, the flow transforms to shear layer mode and self-sustaining oscillations occur. For larger cavities and higher Reynolds and Mach numbers, the flow is transformed to wake mode. A turbulent boundary layer occurring downstream induces backflow into the cavity and gives rise to instability. Rizzetta and Visbel [7] carried out large-eddy simulations over a rectangular pit (L/D = 5) for Mach 1.19. Fourth order compact finite difference scheme approximation was used along with a non-dispersive filter of sixth order to address the spatial derivatives. Experimental data obtained from higher Reynold's number was compared with suppressed and unsuppressed cases. Unalmis et al. [8] did examinations at a greater Reynolds number for Mach number 2 and 5, strong, open cavity stream. A slab was employed to enclose 5/6th of the pit to detach the shear layer from the pit. No particular vibrations on the slab were detected. Vicente et al. [9] illustrated the flowfield loop among shear layer and duct was interrupted, decoupling between cavity acoustics and the shear layer took place. This configuration in incompressible flow has the biglobal instability analysis employed. To solve directly, the compressible biglobal eigenvalue question, the QZ technique was used. Sipp and Lebedev [10] conducted global stability analysis on an open cavity for base and mean flow conditions. For this condition, the mean current prevails strongly unstable nature in terms of eigenmodes. The frequencies are huge, and not perfect over the non-linear uncertain intermittent cavity stream. Bres and Colonius [11] performed two and 3-D direct numerical computations on an to study the nature of compressible flow above the open duct. The length-depth ratio of the cavity remains at 2 and 4. The flow velocity in the duct is smaller than the velocity of free stream. This resulted instability in the duct. Hence, linear stability analysis showcased those 3-D fluctuations create distortions, increasing the recirculating vortical stream inside of duct. Nayal et al. [12] illustrated that the comprehensive behavior of a cavity as a flame holder is altered by the angle of the front slope of the cavity. Improvisation of recirculation zone and appropriate fusion of fuel and air is achieved through a blunt fore-wall. From the point of view of performance, sustainability of the rear wall at a 90-degree ramp angle is required. Nayal and Sahoo [13] analyzed the influence of a pylon placed on a cavity-based flame holder computationally. The ignition is supported due to the distribution of high pressure with the inclusion of pylon. Mounting a pylon increases 14.6% drag on the cavity. Enhancement in the stream size, recirculation, and strength is more favorable in pylon condition for a supersonic cavity-based flame holder. The present authors, Gholap et al. [14] executed a two-dimensional computational analysis to illustrate the preliminary results of the following investigation, to study the flow behavior without and with a wedge impinging an oblique shock on the shear layer. At supersonic Mach 3, the drag experienced by an open cavity nearly doubled when a shock impinged the shear layer passing the open duct with a length-depth ratio of 3. The intent of this research task is to investigate the effect of shock impingement on the shear layer formed over an open duct with the impinging shock waves of varying strength. The cavity considered here is a rectangle, with the ratio for length to depth as 3. The supersonic freestream flow is having Mach number 3. A 2D wedge has been adopted as the shock generator for impingement of the shock wave on the shear layer formed over the cavity. For varying the shock strength, the 2D wedge of various half wedge angles have been adopted in the present study and the shock waves generated on these shock generators are made to impinge on the shear layer. Alteration in the flow physics due to impingement of shock waves of varying strength is analyzed in the present investigation.

2. RESEARCH METHODOLOGY

2.1 Model Geometry

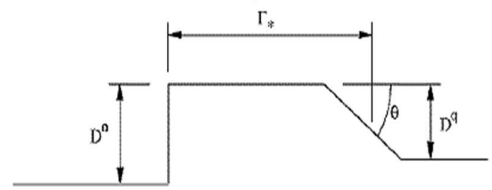

Fig. 2. Schematic of cavity geometry. *Length of the open duct (Gruber et al. 2001).

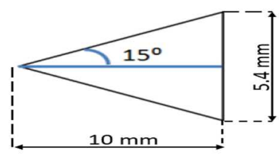

Fig. 3. Typical shock generator for 15°half wedge angles

The basis for the cavity geometry adopted in the present study has been described under the first case (LD3-01-90) of Gruber et al. [5]. The rectangular duct of open type layout has a horizontal span of 26.70 millimetres and an 8.90 millimetres depth. The geometry is 2-D with 90-degree ramp wall angle. Offset ratio (OR) is unity. The cavity layout with general nomenclature has been presented in Figure 2. To generate shock waves, suitable wedge-type shock generators have been adopted with five different half wedge angles starting from 5 degrees to 25 degrees (in the step of 5 degrees). The geometrical details of the shock generator adopted in the present investigation are shown in Figure 3.

To impinge a shock wave into the shear layer over the open duct, the wedge is situated at a height twice the pit's depth. In addition, the shock generator is introduced in such a manner that the base of the shock generator is lined up with the duct's fore wall.

2.2 Computational Solver and Grid Independence Test

The 2D steady-state Navier stokes equations have been solved in the present study with the commercial solver, Ansys-Fluent®. The solver utilizes the turbulent flow k-omega two-equation model. The solver used is explicit-density based including second-order upwinding. For spatial discretization gradient, the algorithm considered was Green Gauss Cell-Based. The nature of mesh adopted is structured for the current investigation, composed of approximately 0.1 million cells. Figure 4 depicts the computational domain adopted for the computations. The adequate mesh has been achieved by conducting suitable solver validation and grid independence study. A medium mesh having the first cell distance equal to 0.0050 mm is considered.

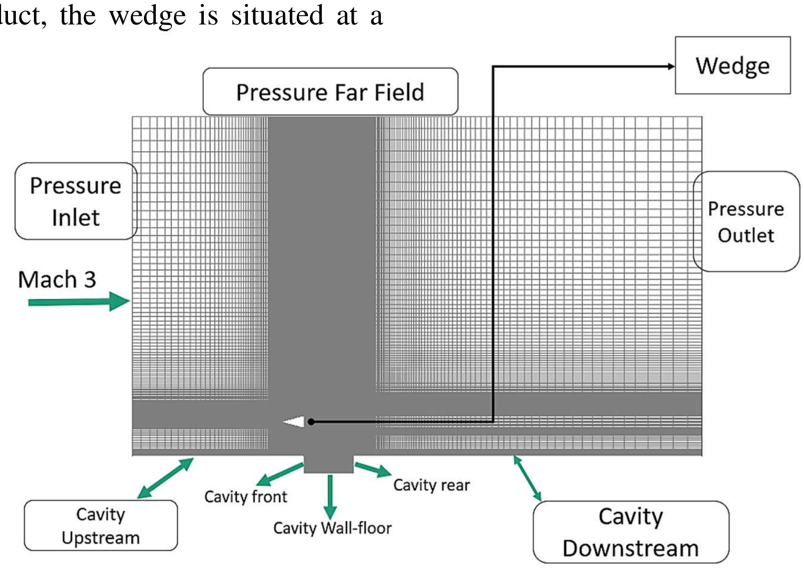

Fig. 4. Domain with a wedge acting as a shock generator to carry out the simulations.

The propriety of the grid was concluded ensuring the converged results achieved with the help grid independence test. The solution quality has been ensured by monitoring the wall Y-Plus values and only after achieving a wall Y-plus value of less than 1, the mesh has been converged for further study. The results were accepted for post-processing only once the residual convergence was found to be below a value of 10^{-5}. The computational domains upper boundary extends up to twenty times the value of pits altitude. The downstream domain expands up to 20 times the cavity height. The upstream is half the upper boundary distance.

The wedge is positioned 17.80 millimeters over the ducts fore wall. The horizontal span of the shock generator results in 10 mm. The downstream domain expands up to 20 times the cavity height. The upstream is half the upper boundary distance. The wedge is positioned 17.80 millimeters over the ducts fore wall. The horizontal span of the shock generator results in 10 mm. The boundaries of the computational domain have been suitably defined, as shown in Figure 4.

2.3 Boundary Conditions

The following boundary conditions have been adopted to conduct the computational simulations in the present investigation. Stagnation pressure and static pressure at the freestream (pressure inlet boundary) are taken to be 690 KPa and 18768 Pa, respectively. Stagnation temperature was maintained at 300 K while the turbulent viscosity ratio and intensity were set to 5 and 0.5 % respectively. The fluid was assumed to be ideal gas and the Sutherland viscosity 3-coefficient model is taken in the current investigation. The freestream temperature on the upper boundary of pressure far-field was 107.16 K. Freestream pressure and Mach numbers were 18768 Pa and 3.0, respectively corresponding to a Reynolds number of 1.8×10^{-5} as per the duct's depth.

3. SOLVER VALIDATION

The computationally and experimentally obtained normalized pressure distribution above the duct surface described in Gruber et al. [5] is considered for validation of the existing solver. The normalized pressure (ratio of the cavity wall static pressure and the freestream pressure) is computed over the total surface span of the rectangular cavity (that is duct fore, floor, and aft wall) in inches. The comparison between the reported (computational and experimental) normalized pressure distribution and the pressure distribution achieved from the current simulation has been depicted in Figure 5. The comparison is found to be a fair match and hence the solver can be considered to be validated. For converging with the suitable grid, five different sets of grid densities have been adopted in the grid independence test ranging from very coarse to the very fine grid. The details of the cell counts adopted in different types of grids and the respective pressure distribution computed over the cavity are shown in Figure 6. From the Figure, a medium grid has been adopted for the present research work.

4. RESULT AND DISCUSSION

The effect of the oblique shock waves strength impinging over the shear layer generated over a cavity is investigated in the present study. The impinging shock waves are generated using a wedge-type shock generator placed at a suitable location over the cavity. To investigate the effect of the strength of the impinging shock wave, the study has been performed at supersonic Mach 3 for the open rectangular cavity with shock impingement prototypes for five different half wedge angles. The variation in the flow physics around the open cavity with the variation in the strength of the impinging shock is computed, analyzed, and reported om the following sub-sections

4.1 Effect on Overall Flowfield

To analyse the effect of the impinging shock wave in the flowfield, the time-averaged Mach contours computed for all the cases of the open cavity with the presence of a shock generator (varying wedge angles) are presented in Figure 7. In the first case, i.e., without shock impingement, there is an absence of any impinging shock and almost an undisturbed shear layer can be observed over the cavity (see Figure 7i). However, a slight penetration of the shear layer inside the duct close by the rear wall, as boundary layer increases in thickness, it can be observed and at duct's end, at the upper stagnation corner, a weak shock is seen to appear. For 5° half wedge angle, a very little effect of the generated oblique shock wave over the cavity shear layer can be seen rectangular open ducts aft wall (see Figure7ii). Due to a smaller half-wedge angle, the shock angle generated allows the weak shock wave to pass over the cavity thereby, missing the impingement over the shear layer**.** However, the impingement does happen but at the downstream of the cavity and hence, it does not possess any distortion. On increase of the half-wedge angle of the shock generator, for 10°, the oblique shock impinges on the shear layer before the ducts aft wall. In this case, a slight lift-up of oblique shock wave generated due to the wedge (shock generator), thereby giving rise to a complicated flow phenomenon in the vicinity of the open duct. In 15° half-wedge shock generator angle, the shock wave becomes stronger and due to a larger shock angle, the shock wave impinges right in the middle of the

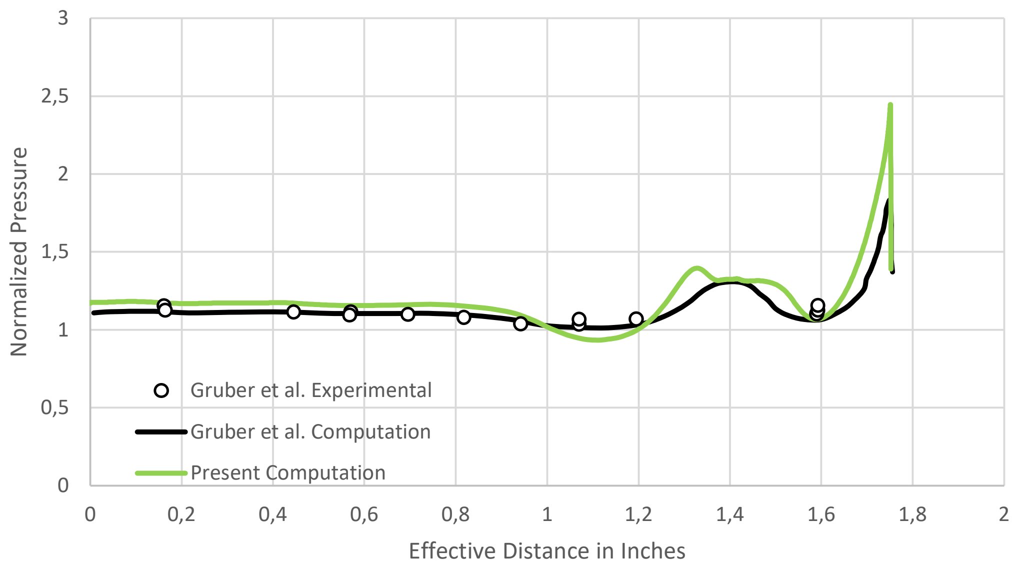

Fig. 5. Affinity of the normalized pressure acting on the walls of the open cavities.

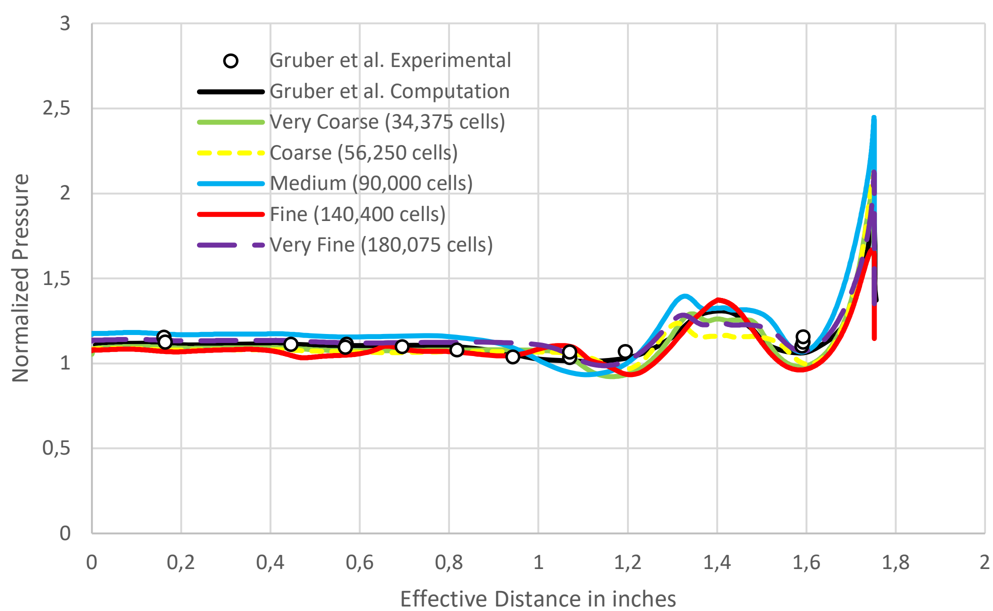

Fig. 6. Grid Independence Test on the open cavity wall.

shear layer is observed as shear layer thickens. Due to the lift up of the shear layer, an additional separation shock wave formation is seen upstream of the cavity (Figure 7iii). This additional separation shock interacts with the pit. Thereby, a stronger interaction among the shear layer and the oblique shock is observed, inducing a higher strength on the cavity. This change in the flow phenomena might lead to an increase in the static pressure distribution over

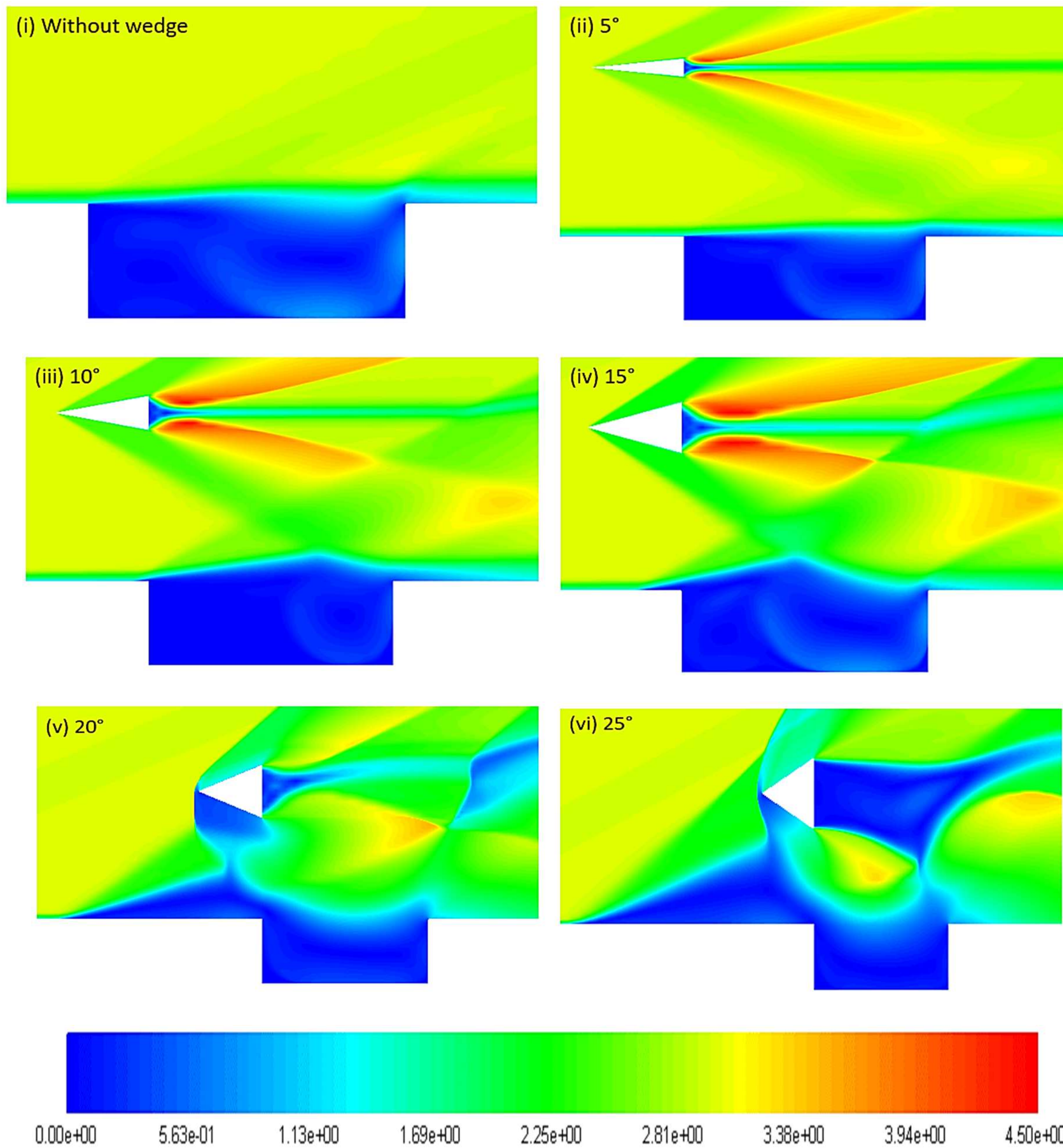

Fig. 7. Mach contours for open cavity with 5-to-25-degree half wedge angles at Mach 3. (The direction of the flow is from leftwards to the right side)

the cavity wall and hence, an increase in the drag can also be expected. The shear layer-shock interaction similar to the previous case can also be seen but the location is more upstream this time (see Figure 7iv). In the 20° half-wedge angle case, the wedge and the upstream cavity wall are also in contact with the shock impingement as a higher wedge angle increases the strength induced on the cavity to a much larger extent. The reflection after hitting the walls is also higher as the shock impinges where the cavity starts and a maximum distortion of flow results in this case (Figure 7v). With higher impinging shock strength, the flowfield around the cavity is observed to be more complex and needs in-depth study in the future. For 25°, the flow trend is similar to that of 20° with a much more complex flow generating in the aft wall portion (See Figure 7vi).

4.2 Effect on the Pressure Distribution over the cavity wall

The effect of the impinging shock wave on normalized pressure distribution (ratio of the static pressure to the freestream pressure) over the duct has been computed and analysed. The variation in the normalized pressure distribution computed for the different cases of the shock wave impingement studies conducted in the present investigation is shown in Figure 8. It can be observed from the Figure that in the absence of the shock wave, the normalized pressure distribution at the duct's floor is found to be on the lower end. However, the level of the normalized pressure distribution in the rectangular pit starts increasing due to the development of compression wave at the duct's separation edge upon shock influencing over the shear layer.

downstream of the duct. The pressure peak is maximum for the 20° case, whereas overall maximum strength on the cavity wall is noticed in the case of 25° half wedge angle. Based on the above analysis from the pressure distribution, an increase in the drag values can also be expected with a rise in the oblique shock wave strength impinging the cavity.

4.3 Drag Coefficient Analysis

Table 1 presents the drag coefficients computed in both with and without impingement of the shock cases. As expected from the previous sub-sections, there is a boost in the drag

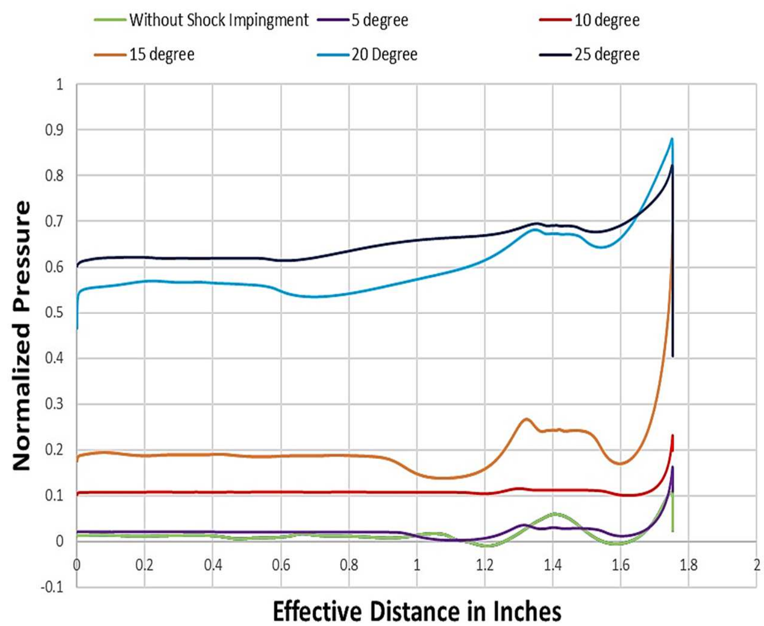

Fig. 8. Normalized pressure distribution along the open cavity for open cavity and with shock impingement cases.

This observation is aligned to the trend expected based on the analysis made from the computed Mach contours in the previous sub-section. The rear wall end of the open rectangular duct encounters recompression shock which leads pressure augmentation. From Figure 8, it can be observed that a pressure peak emerges before an effective length of 1.5 inches which might be due to the existance of the recirculating vortex inside the duct. In considering the case of impingement of shock, the static pressure rises as the half wedge angle increases. There is no major change in the cavity without any shock impingement and the 5° case as the shock wave impinged only at the

coefficient, as given in the data, for the cases with shock impingement. The oblique shock impingement results a greater magnitude of pressure. It reacts on the duct wall, thus increasing the drag force. All the wedge cases are compared with respect to the without shock impingement model. Based on the present analysis, to increase the drag coefficient on the cavity walls, 15°, 20°, and 25° half wedge angles are suitable. With 20° case causing a maximum increase in the drag coefficient value. A 421.80 % increase in the drag coefficient compared to the no wedge case is observed. The pressure distribution on the aft wall corner region of the 20° half wedge angle is also maximum when compared to the rest of the cases. In the 5° and 10° half wedge angle cases, a decrease in drag coefficient is observed. The reason behind this might be because, the shock mostly impinges downstream the cavity disturbing the rear shock, which possesses the maximum magnitude in the rectangular open cavity computations. For 25° case, the drag is not doubled as that of 20°, as the 25° half wedge angle consumes more space, the shock wave hits the cavity in the upstream region and due to a larger surface area of the base, a higher drag can be experienced by the wedge itself. The oblique shock wave hits the wall before the cavity and reflects back causing a minimum intensity on the shear layer which is present above the duct compared to the 20° case. Since 25° has maximum distortion in the flow passing through the cavity, 15° and 20° are more feasible conditions to increase the amount of drag on the cavity. Whereas, 5° and 10° cases are more favourable to reduce the amount of drag occurring on the cavity.

Table 1: Computed drag coefficient values over open cavity without and without shock impingement.

Cases (Half wedge angle)	Drag Coefficient	Increase/Decrease in CD
No wedge	0.000243	
5°	0.0000981	59.63 % decrease
10°	0.0000626	74.24 % decrease
15°	0.000511	110.28% increase
20°	0.00123	421.80% increase
25°	0.000778	220.16% increase

5. CONCLUSION

In the current computational research, the effect on the shear layer due to an oblique shock wave impingement has been investigated. The flowfields have been inspected computationally at a freestream Mach 3 for six different cases i.e., in the existence of impinging shock with varying shock strengths (5 cases) and without impingement of shock. The distribution of pressure and correlation of coefficient of drag has also been evaluated for the effectful length over the duct wall measured in inches. The major conclusions of the present investigation can be listed as follows:

i) The absence of shock impingement shows no disturbance on the shear layer. However, in the situation of shock impingement cases, the form of the shear layer is found to be disturbed. The change in the flow physics leads to a stronger recirculation and a lift-up of the shear layer. The flow is observed to be highly disturbed and a stronger rear shock is generated on the duct's aft wall corner point.

ii) The impingement of shock wave over the shear layer leads to a rise in pressure distribution over the cavity surface. The magnitude of the surface pressure distribution is found to be increasing with the rise of the impinging shock waves strength.

iii) In the existence of shock wave influencing on the shear layer, a greater force is observed to be experienced on the open rectangular duct. For 25° shock impingement case resulted in maximum pressure distribution level. The lowest drag coefficient was illustrated in the 10° case which reported around a 74.24% decrease in comparison to the no shock impingement case. The 20° case caused maximum distortion in the cavity flow field with an 421.80% increase in the C_d value on the cavity wall. The drag force increases by five times due to the impact on the flow field by higher pressure.

REFERENCES

[1] O. Wayne, M., Robert, W., *Drag of Rectangular Cavities in Supersonic and Transonic Flow Including the Effects of Cavity Resonance*, AIAA Journal 1970, 8(11), pp. 1959-1964.

[2] J.A., E., X. Z., *Some Aspects of Supersonic Flow Over a Cascade Flow*, Astrodynamics Conference, August 1986, Williamsburg, VA, USA.

[3] X., Z., J.A., E., *Computational Analysis of Unsteady Supersonic Cavity Flows Driven by Thick Shear Layers*, Aeronautical Journal 1988, Vol. 92(919), pp. 365-374.

[4] O., B., R. L. Jr., S., *Computational and Experimental Investigation of Cavity Flowfields*, AIAA Journal 1988, Vol. 26(1), pp. 6-7.

[5] Mark., G., Robert, B., Tarun, M., K.Y., H., *Fundamental Studies of Cavity-Based Flameholder Concepts for Supersonic Combustors*, Journal of Propulsion and Power, 1988, Vol. 17(1), pp. 146-153.

[6] Clarence, R., Tim, C., Amit, B., *On Self Sustained Oscillations in Two-Dimensional Compressible Flow Over Rectangular Cavities*, J. Fluid Mechanics, 2002, Vol. 455, pp. 315-346.

[7] Donald, R., Miguel, V., *Large-Eddy Simulation of Supersonic Cavity Flowfields Including Flow Control*, AIAA Journal, 2003, Vol. 41(8), pp. 1452-1462.

[8] Omer, U., Noel, C., D., D., *Cavity Oscillation Mechanisms in High-Speed Flows,* AIAA Journal, 2004, Vol. 42(10), pp. 2035-2041.

[9] Javier de, V., Eusebio, V., Leo, G., Vassilios, T., *Spectral Multi-Domain Methods for BiGlobal Instability Analysis of Complex Flows over Open Cavity Configurations*, 36th AIAA Fluid Dynamics Conference and Exhibit, 2006, San Francisco, California, USA.

[10] Denis, S., Anton, L., *Global Stabilityof Base and Mean Flows: A General Approach and its Applications to Cylinder and Open Cavity Flows*, J. Fluid Mechanics 2007, Vol. 593, pp. 333-358.

[11] Guillaume, B., Tim, C., *Three Dimensional Instabilities in Compressible Flows Over Open Cavity*, J. Fluid Mechanics 2008, Vol. 559, pp. 309-339.

[12] Sanchayata, N., Sampada, L., Devabrata, S., Nandagiri, R., S.A.I., B., *Computational Analysis of Novel Cavity-Based Flameholder Designs for Supersonic Combustion Engines*, IOP Conference Series: Material Science and Engineering, January 2020, Vol. 814, Pandharpur, Maharashtra, India.

[13] Sanchayata, N., Devabrata, S., *Effect of a Pylon Mounted Cavity-Based Flameholder on the Combustor Flow Characteristics*, Journal of Applied Fluid Mechanics 2021, Vol. 14(6), pp. 1635-1642.

[14] Tanmay, G., Majella, R., Adithya, M., Deepthi, B., Devabrata, S., *A Two-Dimensional Computational Analysis Over an Open Cavity with a Shock Impingement*, IEEE Pune Section International Conference December 2021, pp.1-5.

ANALIZA COMPUTAȚIONALĂ A FIZICII DECURSULUI PENTRU O CAVITATE DESCHISĂ DREPTUNGULARĂ CU IMPINGEMENTURI DE ȘOC VARIATIVE

Rezumat: În aviație, cavitățile deschise au un rol critic în influențarea caracteristicilor de performanță. Componentele precum camera de combustie, trenul de aterizare și compartimentele pentru arme conțin o cavitate influențată de stratul de forfecare. Condițiile supersonice ale fluxurilor de cavitate sunt o condiție prealabilă pentru configurarea rachetelor și a viitoarelor vehicule aerospațiale. În cercetarea de față, fluxul care trece deasupra unei cariere dreptunghiulare care conține un strat de forfecare este studiat computațional după impactul unei unde de șoc oblice generată de un generator de șoc tip pană. Conducta cavitară investigată în studiul de față are un raport lungime/adâncime de 3 la unghiul de atac de zero grade. Investigarea asupra influenței caracteristicilor de curgere, cum ar fi mărimea rezistenței, distribuția presiunii și recirculația în interiorul conductei a fost efectuată și analizată pentru cazurile în care există și absența generatorului de șoc la Mach 3. Nu apare nicio întrerupere specială a stratului de forfecare în absența unui șoc oblic. Cu toate acestea, se observă o recirculare robustă în cazurile de impact de șoc. Stratul de forfecare se ridică din cauza forței de împingere generată în cavitatea deschisă la impactul unei unde de șoc. Un șoc puternic din spate este generat în punctul de separare a peretelui din spate al conductei deschise. Mai mult, este investigat și efectul creșterii forței șocului de impact asupra întregului flux peste cavitate. Pe măsură ce puterea șocului de impact crește, s-a observat că și mărimea distribuției presiunii pe suprafața cavității crește.

Tanmay B. GHOLAP, Engineering Student, Annasaheb Dange College of Engineering and Techonology, Ashta, Aeronautical Engineering, tanmaygholap@gmail.com, Phone: +91-7888268190, Plot no. 10, Raju Baba Colony, Old Khandala road, Lonavala, District: Pune-410401, Maharashtra, INDIA.

Majella Riona R., Engineering Student, Sathyabama Institute of Science and Technology, Aeronautical Engineering, majellariona@gmail.com, Phone: +91-9841596704, 6, 4th Main Road, Kamraj Nagar, Thiruvanmiyur, Chennai, INDIA.

Adithya M., Engineering Student, Sathyabama Institute of Science and Technology, Aeronautical Engineering, adithyamagesh@gmail.com, Phone: +91-9952949849, E51A/1A Ramaniyam Orchid 16th Cross Street, Besant Nagar, Chennai, INDIA.

Deepthi Chowdary BOLLA, Engineering Student, Sathyabama Institute of Science and Technology, Aeronautical Engineering, deepthibolla0@gmail.com, Phone: +91-9346082868, 2-82, Main Road, Next to Petrol Bunk, Nagullanka, East Godavari District, Andhra Pradesh, INDIA.

Devabrata SAHOO, Ph. D. Eng., Associate Professor, MIT School of Engineering, MIT ADT University, Aerospace Engineering, devtapu@gmail.com, Phone: +91-6372992092, B2-505, GrandBay, Survey No. 65, Solapur- Pune Hwy, Next to Shewalwadi Octroi Naka, Manjri Bk, Pune, Maharashtra-412307, INDIA.